

This article was downloaded by:

On: 25 January 2011

Access details: *Access Details: Free Access*

Publisher *Taylor & Francis*

Informa Ltd Registered in England and Wales Registered Number: 1072954 Registered office: Mortimer House, 37-41 Mortimer Street, London W1T 3JH, UK



Separation Science and Technology

Publication details, including instructions for authors and subscription information:

<http://www.informaworld.com/smpp/title~content=t713708471>

Mathematical Modelling of Particle Removal and Head Loss in Rapid Gravity Filtration

Shejiao Han^a; Caroline S. B. Fitzpatrick^a; Andrew Wetherill^b

^a Department of Civil & Environmental Engineering, University College, London, UK ^b Yorkshire Water, Bradford, UK

To cite this Article Han, Shejiao , Fitzpatrick, Caroline S. B. and Wetherill, Andrew(2008) 'Mathematical Modelling of Particle Removal and Head Loss in Rapid Gravity Filtration', *Separation Science and Technology*, 43: 7, 1798 – 1812

To link to this Article: DOI: 10.1080/01496390801973631

URL: <http://dx.doi.org/10.1080/01496390801973631>

PLEASE SCROLL DOWN FOR ARTICLE

Full terms and conditions of use: <http://www.informaworld.com/terms-and-conditions-of-access.pdf>

This article may be used for research, teaching and private study purposes. Any substantial or systematic reproduction, re-distribution, re-selling, loan or sub-licensing, systematic supply or distribution in any form to anyone is expressly forbidden.

The publisher does not give any warranty express or implied or make any representation that the contents will be complete or accurate or up to date. The accuracy of any instructions, formulae and drug doses should be independently verified with primary sources. The publisher shall not be liable for any loss, actions, claims, proceedings, demand or costs or damages whatsoever or howsoever caused arising directly or indirectly in connection with or arising out of the use of this material.

Mathematical Modelling of Particle Removal and Head Loss in Rapid Gravity Filtration

Shejiao Han,¹ Caroline S. B. Fitzpatrick,¹
and Andrew Wetherill²

¹Department of Civil & Environmental Engineering, University College London, UK

²Yorkshire Water, Bradford, UK

Abstract: A new filtration model has been developed to describe the entire three-stage filtration run. The two-stage assumption is applied for physical description of the rapid gravity filtration process. At the first stage of the filtration, previously deposited particles serve as collectors to improve particle removal efficiency and the detachment of deposited particles does not occur until the specific deposit reaches a certain transient specific deposit where the second stage starts. Particle detachment rate at the second stage is assumed to be a function of relative specific deposit and hydrodynamic conditions within filter media. The proposed filtration model has been applied to fit the data from one water treatment plant of Yorkshire Water (UK). The comparison demonstrates a good agreement between water treatment site data and the simulated results.

Keywords: Rapid gravity filtration, modelling, particle removal, head loss

INTRODUCTION

Rapid gravity filtration is a commonly used solid/liquid separation process for drinking water treatment. Mathematical models with predictive capabilities are important tools for the design and operation of rapid gravity filters.

Received 4 June 2007, Accepted 13 December 2007

Address correspondence to Caroline S. B. Fitzpatrick, Department of Civil & Environmental Engineering, University College London, Gower Street London WC1E 6BT, UK. Tel.: +44 (0) 20 7679 2689; Fax: +44 (0) 20 7380 0986; E-mail: c.fitzpatrick@ucl.ac.uk

In order to have good predictability of filter performance, it is essential to understand mechanisms underlying the rapid gravity filtration process. In terms of effluent concentration changes, an entire filtration run is usually divided into three stages, described as ripening, working, and breakthrough. The improvement in particle removal efficiency is known as ripening at the start of the filtration run. The characteristics of bed ripening are a major concern in the design and operation of rapid gravity filters. O'Melia and Ali (1) investigated the effects of previously deposited particles on the changes of removal efficiency and head loss that occur with time on the ripening stage, and a model was proposed to describe the removal efficiency of a collector that consists of a filter grain and an associated number of particles deposited to it that also serve as collectors. It should be noted that the model developed by (1) is limited to the ripening stage. Their work was then extended by a number of other researchers (2–4). At the working stage the filter possesses a stable removal capability so that the effluent concentrations remain stable at low levels. Following the working stage, the effluent concentration starts to increase until the whole filter loses its separation capacity. Obviously, another concern with design and operation of rapid gravity filters is breakthrough where the effluent quality starts to deteriorate and the filtration operation has to stop for backwashing for the next filtration run. It has been experimentally observed that the detachment of already deposited particles on the grains is an important phenomenon during the filtration that brings deposited particles from the top to the bottom of the filter causing breakthrough (5–7). Adin and Rebhun (5) proposed a rate expression that includes a second term to consider detachment of already deposited particles, i.e.

$$\frac{\partial \sigma}{\partial t} = k_1 u c (F - \sigma) - k_2 \sigma J \quad (1)$$

It should be noted that Equation (1) is not applicable for the ripening stage.

In this study, a filtration model will be established to describe the entire filtration run consisting of ripening, working and breakthrough three stages. The proposed filtration model will be applied to fit the filter effluent turbidity data from one water treatment Yorkshire Water plant in the UK.

DEVELOPMENT OF A FILTRATION MODEL

Physical Descriptions of the Filtration Model

Tien et al. (8) proposed that the filtration process consists of two consecutive stages, i.e. a smooth coating mode followed by the constriction clogging mode. In this study, the two-stage hypothesis is also applied to describe the entire rapid gravity filtration process but a different approach will be taken:

Stage 1: Suspended particles start to deposit outside filter grains and previously deposited particles begin to serve as additional collector sites for the further attachment of suspended particles. The detachment of deposited particles does not occur during filtration at this period of time until the specific deposit reaches a certain value σ_c . This assumption is consistent with experimental observations carried out by Ives (6). First Ives (6) used endoscopes with video recording inserted into rapid sand filters to observe directly and dynamically filtration deposition in the filter pores. It was revealed in his experiments that deposits of clay over grains accumulated over several hours of filtration, then were partially detached by the arrival of further suspension particles. It was concluded in his work that detachment during filtration is a real phenomenon, but only when substantial deposits are present.

Stage 2: The detachment starts to occur, mainly due to the increase of hydraulic shear forces with increase of interstitial velocity within the free space of filter media. The detachment phenomenon has been observed and simulated by a number of researchers (5–7, 9). At the second stage both deposition and detachment take place.

Mass Balance within the Filter Column

The mass conservation of particles within the filter in the filtration can be written by

$$\frac{\partial(\varepsilon c)}{\partial t} + V \cdot \nabla(\varepsilon c) - \nabla(\varepsilon D \nabla c) + \frac{\partial \sigma}{\partial t} = 0 \quad (2)$$

For a randomly packed granular filter with a rather large ratio of bed diameter to granule diameter, the flow along the filter column is usually assumed a plug flow and the dispersion term is negligible. And the change in pore-suspension concentration with time is also negligible compared to the change in the specific deposit (5, 8). Therefore, the mass balance within the filter can be simplified as

$$u \frac{\partial c}{\partial z} + \frac{\partial \sigma}{\partial t} = 0 \quad (3)$$

For filtration with a clean filter, the initial and boundary conditions can be defined as

$$c = 0, \sigma = 0 \quad \text{for } z \geq 0, t = 0 \quad (4)$$

$$c = c_{in} \quad \text{for } z = 0, t > 0 \quad (5)$$

It can be obviously seen from Equation (3) that the deposition rate needs to be determined for predicting the changes of suspended particle and specific deposit concentrations in time and space.

Deposition Rates at Two Stages

Iwasaki (10) first proposed a rate expression that describes a first-order removal with depth proportional to the local particle concentration in the fluid

$$\frac{\partial c}{\partial z} = -\lambda c \quad (6)$$

Assuming that filter grains are perfect spheres, the number of collectors in the differential volume with a height dz and a cross-section area A_c can be calculated by

$$N_c = \frac{6(1 - \varepsilon_0)A_c dz}{\pi d_c^3} \quad (7)$$

By the definition that the single collector removal efficiency η is the ratio of the rate at which particles deposit on the collector divided by the rate at which particles flow toward the collector, the mass conservation of particles in the volume element can be written as (11)

$$\frac{3}{2} \eta(1 - \varepsilon_0) \frac{u}{d_c} c A_c dz = -(u A_c) dc \quad (8)$$

Comparing Equations (6) and (8) gives

$$\lambda = \frac{3(1 - \varepsilon_0)\eta}{2 d_c} \quad (9)$$

As mentioned in the Introduction, O'Melia and Ali (1) proposed that at the ripening stage the actual collector consists of a filter grain and an associated number of particles deposited to it that also serve as collectors, and the removal efficiency of the single collector was calculated by

$$\eta = \alpha \eta_0 + N \alpha_p \eta_p \left(\frac{d_p}{d_c} \right)^2 \quad (10)$$

and

$$N = \alpha \eta_0 \beta \left(\frac{3}{2 \times (1000 \times \rho_p) d_p^3} \frac{d_c^2}{d_p^2} \right) u \int_0^t c dt \quad (11)$$

The following correlation developed by Rajagopalan and Tien (12) is applied for the calculation of η_0

$$\eta_0 = 4.0 A_s^{1/3} \left(\frac{D_\infty}{u d_c} \right)^{2/3} + A_s N_{LO}^{1/8} N_R^{15/8} + 3.38 \times 10^{-3} A_s N_G^{1.2} N_R^{-0.4} \quad (12)$$

where $A_s = 2(1 - p^5)/w$, $w = 2 - 3p + 3p^5 - 2p^6$ and $p = (1 - \varepsilon)^{1/3}$.

The deposition rate at the first stage of the filtration can be obtained by combining Equations (3), (6) and (9–11).

$$\frac{\partial\sigma}{\partial t} = \frac{3(1-\varepsilon)}{2d_c} \alpha\eta_0 \left[1 + \alpha_p\eta_p\beta \left(\frac{3}{2 \times (1000 \times \rho_p)} \frac{d_c^2}{d_p^3} \right) u \int_0^t c dt \right]$$

$$uc \quad \sigma \leq \sigma_c \quad (13)$$

As mentioned earlier, experimental observations carried out by Ives (6) indicated that detachment does not occur until substantial deposits are present in the filter, represented by a certain value of σ_c . This suggests that deposited particles forming this amount of accumulated material will not be detached by fluid shear forces during entire filtration. Therefore, the detachment rate is assumed to be proportional to the relative specific deposit $\sigma - \sigma_c$ rather than the absolute specific deposit σ , which has been applied by a few researchers to describe the detachment rate (5, 13, 14). The detachment rate is also assumed to be proportional to the hydraulic gradient within the filter media. The following equation is proposed to describe the deposition rate at the second stage of the filtration

$$\frac{\partial\sigma}{\partial t} = \frac{3(1-\varepsilon)}{2d_c} \left[\alpha\eta_0 + \alpha_p\eta_p\beta \left(\frac{d_p}{d_c} \right)^2 N \right] uc - \varpi J(\sigma - \sigma_c) \quad \sigma > \sigma_c \quad (14)$$

where

$$N = \alpha\eta_0 \left(\frac{3}{2 \times (1000 \times \rho_p)} \frac{d_c^2}{d_p^3} \right) \int_0^{t_c} uc dt$$

$$+ \int_{t_c}^t \frac{1}{1000 \times \rho_p(1-\varepsilon_0)} \left(\frac{d_c}{d_p} \right)^3 \frac{\partial\sigma}{\partial t} dt \quad (15)$$

N is an associated number of deposited particles which are served as additional collectors for a single filter grain. The first term and the second term on the right side of Equation (15) represent the number of deposited particles at the first and second stages respectively.

The experimental data obtained by Adin, and Rebhun (5) suggested that the detachment coefficient ϖ could be described as a function of filtration flow rate. The following expression was obtained in their study:

$$\varpi = \varpi_0 u^{1.75} \quad (16)$$

ϖ_0 is a constant for a specific filtration system.

Head Loss through the Filter Column

Under the condition with a constant filtration flow rate, the deposition of suspended particles on the surface of filter media causes the clogging, resulting in the reduction of permeability. O'Melia and Ali (1) proposed that permeability is inversely proportional to the square of interfacial surface area in the filter. On the basis of this assumption, Mays and Hunt (15) developed the following equation for the calculation of hydraulic gradient within a clogged filter

$$J = J_0 \left(1 + \frac{\gamma}{\rho_p} \sigma \right)^2 \quad (17)$$

γ is an empirical parameter which is related to the flow rate, the particle surface area to volume ratio, filter grain size, and clean filter bed porosity. And on the basis of experimental data in the literature, γ was proposed to be expressed as

$$\gamma = \gamma_0 u^{-0.55} \quad (18)$$

γ_0 is a constant for a specific filtration system.

Combining Equations (17) and (18) gives

$$J = J_0 \left(1 + \frac{\gamma_0}{\rho_p} u^{-0.55} \sigma \right)^2 \quad (19)$$

Therefore, the head loss through the filter can be calculated by

$$h = J_0 \int_0^L \left(1 + \frac{\gamma_0}{\rho_p} u^{-0.55} \sigma \right)^2 dz \quad (20)$$

Suspended particle concentration and specific deposit profiles within the filter in time and space can be simulated by solving Equations (3–5), (13) and (14). The head loss through the filter is calculated by Equation (20). The hydraulic gradient in the clean filter bed J_0 can be calculated by the Carman-Kozeny equation or be experimentally obtained.

RESULTS AND DISCUSSION

Model Simulation

Model Parameters

The parameters to be determined include α , α_p , η_p , β , ϖ_0 , σ_c , and γ_0 in the proposed filtration model. Since the parameters of α_p , η_p , and β are present

as a group in the model, these can be treated as a single parameter. Use of this model requires specification of values for these model parameters.

As described by O'Melia and Ali (1), particle removal (c_e/c_{in}) from the clean bed to the end of ripening stage is controlled by the values of α and α_p , η_p , β . α values are in the range of 0.5–1 for favorable chemical conditions (4). α values can be calculated from the experimental data for clean or initial filter bed particle removal. The value of α_p , η_p , β is estimated by best fitting experimental data with the calculated values of particle removal efficiency at ripening stage in the proposed filtration model. In similar manner, the values of ϖ_0 and σ_c can be estimated by particle removal at breakthrough stage. Head loss coefficient γ_0 is determined by best fitting experimental results with the simulated head loss profile in the proposed filtration model.

The filtration model is numerically solved to simulate suspended particle concentration and specific deposit profiles within the filter column in the filtration (Filtration time is assumed to be 24 hours for this simulation). This information will help to understand what happens within the filter column during filtration.

In the simulation, the filter column with a depth of 0.9 m is divided into 100 layers. The values of model parameters were deliberately chosen to make breakthrough take place significantly, so that the proposed filtration model can be fully assessed. The values of model parameters for the simulation are listed in Table 1.

Suspended Particle Concentration and Specific Deposit Profiles within the Filter Column

Figure 1 shows relative suspended particle concentration profiles with filter depth during the 24 hour filtration. It can be seen that the particle concentration rapidly declines with depth at the top of the filter, indicating that effective particle removal is achieved. After 2 hour filtration, there is little reduction in the suspended particle concentration over the top layers of about 0.05 m, but the particle concentration continues to decrease at lower layers. This means that the top layers of the filter start to lose separation capability but particle removal is still improved over the rest of the filter column. With further filtration operation, the reduction and even complete loss of

Table 1. The values of model parameters for the simulation

$L = 0.9$ m	$\alpha = 0.9$
$c_{in} = 6$ mg/L	$\alpha_p, \eta_p, \beta = 0.9$
$u = 5$ m/hr	$\varpi_0 = 200$
$d_c = 0.8$ mm	$\sigma_c = 300$ mg/L
$d_p = 4$ μ m	$h_0 = 0.4$ m
$\varepsilon_0 = 0.4$	$\gamma_0 = 30$

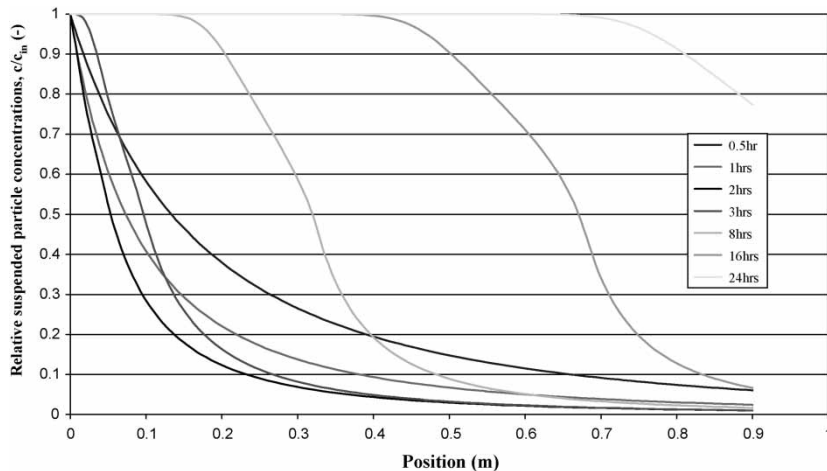


Figure 1. Relative suspended particle concentration profiles along the filter column at various filtration times.

separation capability takes place from the top to the lower part of the filter. These simulated particle concentration profiles are consistent with experimental results obtained by Deb (16) and Hunt et al. (17). It should be pointed out that the suspended particle profiles for 0.54 mm sand did not demonstrate the ripening stage in the work carried out by Hunt et al. (17). This may be because in experimental measures conducted by Hunt et al. (17), samples were taken after 30 minutes from the start of filtration runs. But the ripening stage could be very short for this fine size sand.

The simulated results in Fig. 1 illustrate that after 24 hour filtration effluent concentration reaches 70–80 percent of the influent concentration, and about 0.7 m upper part of 0.9 m filter column has completely lost the separation capacity. Thus it can be explained that the upper layers play a major role in particle removal at the beginning of filtration. As deposits build up, the velocities increase through the more clogged upper layers of the filter, enhancing particle detachment. Therefore, these layers become less effective in particle removal. The burden of particle removal passes deeper and deeper from the top to the bottom into the filter. Once the removal capacity deteriorates within the bottom layers of the filter, the effluent concentration will start to increase until the whole filter possesses no separation capacity.

As shown in Fig. 2, specific deposit declines with filter depth. The occurrence of the fluctuation of specific deposit profiles is caused by numerical simulation. As deposits build up with filtration, specific deposit through the filter column increases with filtration time, with a more significant increase at the upper layers. After 3 hour filtration, the very top layers start to be

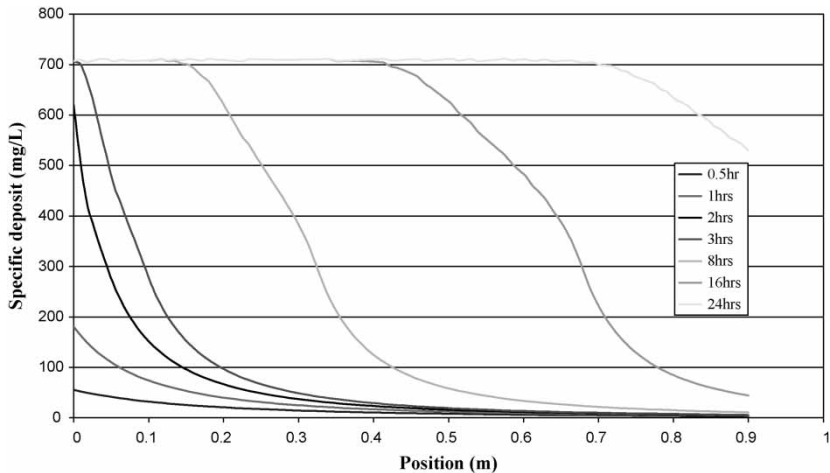


Figure 2. Specific deposit profiles along the filter column at various filtration times.

saturated with a specific deposit of around 700 mg/L. This indicates that this part of the filter has completely lost its separation capacity. Further filtration brings more filter column saturated. These simulated specific deposit profiles along the filter column demonstrate the trends of the experimental results obtained by Hunt et al. (17). However, in their experimental tests, the peaks of specific deposit occurred at an upper layer after the filtration ran for a while. But there was no explanation given for these results.

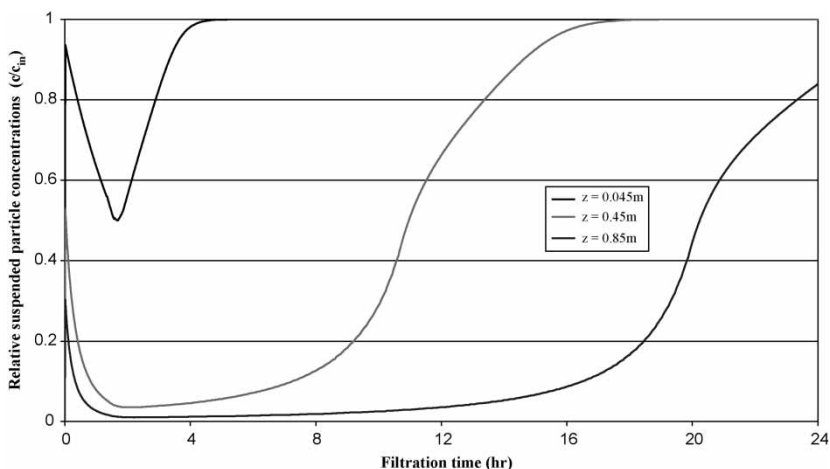


Figure 3. Relative suspended particle profiles with filtration time at different positions.

Figure 3 illustrates the changes in suspended particle concentration with filtration time at the upper, middle and lower layers ($z = 0.045$ m, 0.45 m, and 0.85 m) along the filter column. It can be seen that the particle concentrations in the upper layer ($z = 0.045$ m) are always high during filtration and breakthrough occurs quickly. Proceeding downwards though the filter column ($z = 0.45$ m and 0.85 m), the breakthrough is delayed and the suspended particle concentrations in the working stage get lower and lower. These simulated suspended particle concentration profiles are consistent with the experimental results obtained by Adin and Rebhun (5). In their work, suspended particle concentrations were measured at different filtration times at eight different positions from the top of the filter column. As shown in the Fig. 9 in the reference, suspended particle concentrations at two top positions ($z = 0.05$ m and 0.10 m) were always higher than a half of the influent concentration and the breakthrough rapidly started after the ripening stage took place. At the bottom position ($z = 1.0$ m), quite low particle concentrations were obtained for a long period of time at the working stage, even without a clear breakthrough at the end of test.

Although suspended particle concentrations keep at the high level at the upper layer, the specific deposits increase rapidly at the layer before the filter media is saturated at around 700 mg/L, as shown in Fig. 4. Specific deposits increase much slowly at the lower layers ($z = 0.45$ m and 0.85 m). This demonstrates that the upper layers play a major role in particle removal and the bed depth is also essential to achieve low particle concentrations in the effluent. The simulated specific deposit profiles shown in Fig. 4 are consistent with the experimental results obtained by Ives (18).

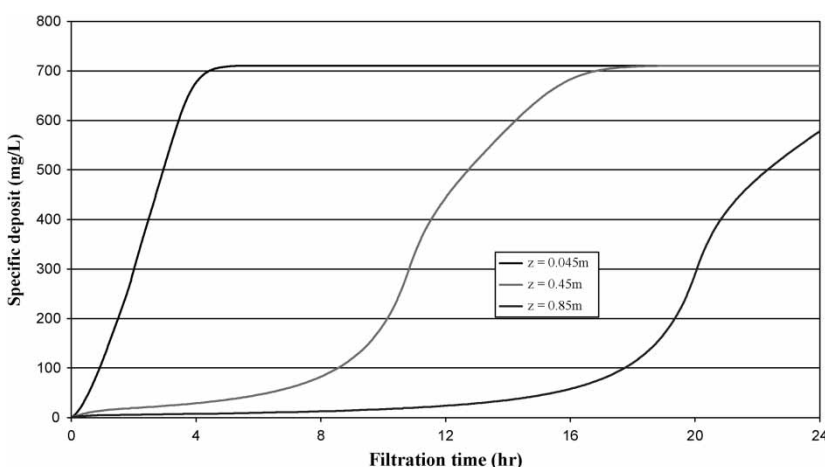


Figure 4. Specific deposit profiles with filtration time at different positions.

Effluent Particle Concentration and Head Loss through the Filter Column

Figure 5 shows the effluent concentration profile with filtration time. The simulated results clearly demonstrate a typical pattern of the effluent concentrations, which consists of ripening, working and breakthrough stages. Head loss through the filter increases with filtration time, as also shown in Fig. 5. After about 21 hour filtration, the increase in head loss of filter media starts to slow down. This is because most part of the filter has been saturated, as discussed earlier.

The Effect of Flow Rate on Filter Separation Capability

Three different flow rates were chosen to simulate effluent concentrations at these flow rates. As illustrated in Fig. 6, effluent concentrations significantly increase with increase in flow rate, although the effect of the flow rate on effluent concentration can be exaggerated in this simulation. This may be due to the fact that the increase in flow rate will enhance the detachment of already deposited particles from the filter grains, as described in the filtration model. Presumably, the saturated specific deposit decreases with the increase in flow rate, as shown in Fig. 7. This data is consistent with observations in Yorkshire Water (UK) treatment plants. This suggests that a high flow rate is not recommended in the rapid gravity filtration.

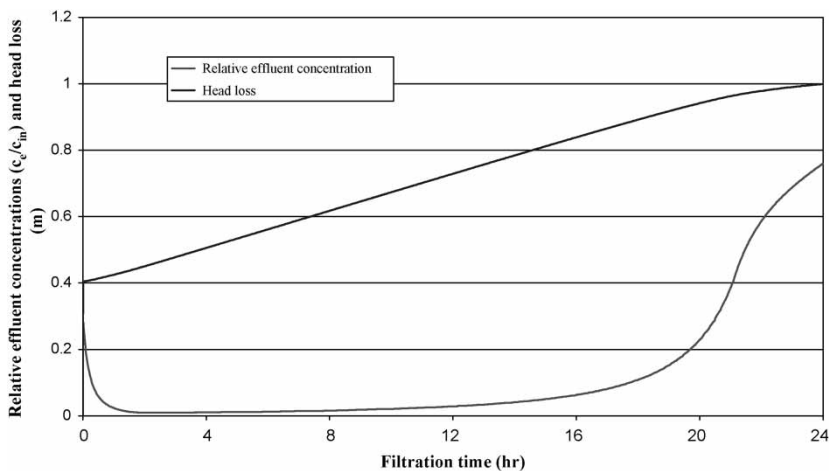


Figure 5. Relative effluent concentrations and head loss through the filter column during the filtration.

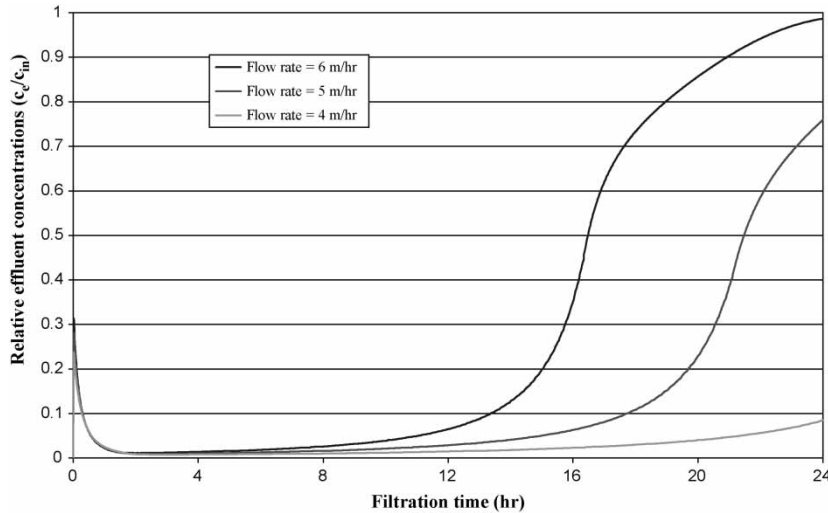


Figure 6. The effect of flow rates on relative effluent concentrations.

Comparison of Simulated Results with Data from a Full Scale Water Treatment Plant

Figure 8 shows the data of particle removal and head loss in two runs at one water treatment plant of Yorkshire Water (UK). The filter column is 0.9 m in depth with a cross area of 90 m^2 on this water treatment plant. The sand has a

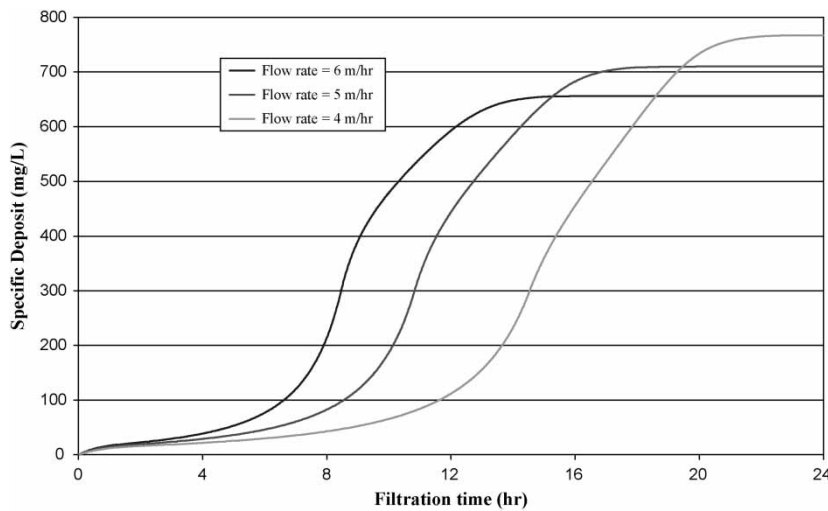


Figure 7. The effect of flow rates on specific deposit at the position of 0.45 m.

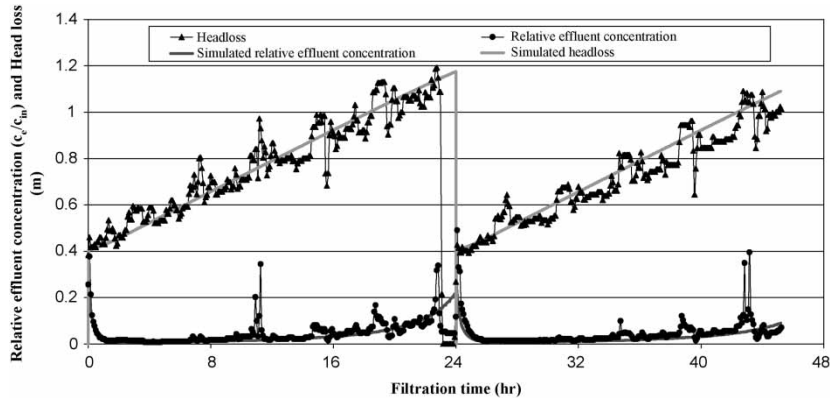


Figure 8. Comparison of simulated results and data from one water treatment plant of Yorkshire Water (UK). $\alpha = 0.9$; α_p , η_p , $\beta = 0.85$; $\varpi_0 = 260$; $\sigma_c = 600$ mg/L and $\gamma_0 = 35$.

geometric mean size of 0.75 mm with a range of 0.55–1.0 mm, used as filter media. The clean bed porosity is assumed to be 0.4. Influent concentration is 6 mg/L with a suspended particle size of around 4 μm and a density of 1350 g/m³. The operating temperature is around 5°C in filtration.

The proposed filtration model is applied to fit the data from this water treatment plant of Yorkshire Water (UK). The values of model parameters are listed underneath Fig. 8. The comparison shows that the particle removal and head loss can be well described by the proposed filtration model.

Experimental study in a pilot plant will be carried out to independently define the values of model parameters and the model will be further evaluated.

CONCLUSIONS

A new filtration model has been proposed to describe a filtration cycle consisting of ripening, working, and breakthrough stages. The comparison demonstrates a good agreement between water treatment site data and the simulated results from the proposed filtration model. It can be concluded from this preliminary study that this model is capable of prediction of particle removal and head loss during rapid gravity filtration. However, further study will be carried out to calibrate the model parameters and evaluate the model.

NOMENCLATURE

A	Hamaker constant (1×10^{-20} J)
A_c	cross-section area (m ²)

A_s	parameter defined by Equation (12)
c	particle concentration (mg/L)
c_e	effluent particle concentration (mg/L)
c_{in}	influent particle concentration (mg/L)
d_c	clean grain diameter (m)
d_p	particle diameter (m)
D	particle dispersion coefficient (m^2/s)
D_∞	bulk particle diffusion coefficient (m^2/s)
F	theoretical filter capacity (mg/L)
h	head loss (m)
J	hydraulic gradient (-)
J_0	clean bed hydraulic gradient (-)
k_1	attachment coefficient (m^2/g)
k_2	detachment coefficient (1/s)
L	filter bed depth (m)
N_c	number of collectors in filter bed with a height, defined by Equation (7)
N_G	gravitational force number given by $(\rho_p - \rho)gd_p^2/(18 \mu u)$
N_{LO}	dimensionless van der Waals number given by $4A/(9 \pi \mu d_p^2 u)$
N_R	dimensionless ratio of particle to collector size given by d_p/d_c
p	parameter defined by Equation (12)
t	time (s)
t_c	filtration time when the specific deposit reaches the value σ_c
u	superficial velocity (m/s)
z	position in the filter bed (m)
V	fluid velocity (m/s)

Greek Symbols

α	particle/filter grain attachment efficiency (-)
α_p	particle/particle attachment efficiency (-)
β	factor of particles deposited on the filter grain which act as additional collectors (-)
γ	parameter defined by Equation (18)
γ_0	constant (-)
ε	filter medium porosity (-)
ε_0	porosity in clean filter bed (-)
η	particle/filter grain removal efficiency (-)
η_0	particle/filter grain transport efficiency in the clean filter bed (-)
λ	filter coefficient (-)
μ	water viscosity ($\text{Pa} \cdot \text{s}$)
ρ_p	particle density (kg/m^3)
σ	specific deposit (mg/L)
σ_c	transitional specific deposit (mg/L)
ϖ	detachment coefficient (1/s)
ϖ_0	constant (1/s)

ACKNOWLEDGMENTS

The authors gratefully acknowledge funding provided by Engineering and Physical Sciences Research Council (EPSRC), UK and Yorkshire Water, under the Engineering Doctorate program.

REFERENCES

1. O'Melia, C.R. and Ali, W. (1978) The role of retained particles in deep bed filtration. *Prog. Water Tech.*, 10 (5/6): 167.
2. Vigneswaran, S. and Tulachan, R.K. (1988) Mathematical modelling of transient behaviour of deep bed filtration. *Water Res.*, 22 (9): 1093.
3. Darby, J.L., Attanasio, R.E., and Lawler, D.F. (1992) Filtration of heterodisperse suspensions: Modeling of particle removal and head loss. *Water Res.*, 26 (6): 711.
4. Tobiason, J.E. and Vigneswaran, B. (1994) Evaluation of a modified model for deep bed filtration. *Water Res.*, 28 (2): 335.
5. Adin, A. and Rebhun, M. (1978) A model to predict concentration and head loss Profiles in filtration. *J. Am. Water Works Assoc.*, 69 (8): 444.
6. Ives, K.J. (1989) Filtration studied with endoscopes. *Water Res.*, 23 (7): 861.
7. Kim, J. and Tobiason, A. (2004) Particles in filter effluent: The roles of deposition and detachment. *Environ. Sci. Technol.*, 38 (22): 6132.
8. Tien, C., Turian, R.M., and Pense, H. (1979) Simulation of the dynamic behaviour of deep bed filters. *AIChE J.*, 25 (3): 385.
9. Adin, A. and Rebhun, M. (1987) Deep-bed filtration: accumulation-detachment model parameters. *Chem. Eng. Sci.*, 42 (3): 1213.
10. Iwasaki, T. (1937) Some notes on sand filtration. *J. Am. Water Works Assoc.*, 29 (10): 1591.
11. Tien, C. (1989) *Granular Filtration of Aerosols and Hydrosols*; Butterworth: Boston, Massachusetts.
12. Rajagopalan, R. and Tien, C. (1976) Trajectory analysis of deep bed filtration with the sphere-in-cell porous media model. *AIChE J.*, 22: 523.
13. Harvey, R.W. and Garabedian, S.P. (1991) Use of colloid filtration theory in modelling movement of bacteria through a contaminated sandy aquifer. *Environ. Sci. Technol.*, 25 (1): 178.
14. Hendry, M.J., Lawrence, J.R., and Maloszewski, P. (1997) The role of sorption in the transport of *Klebsiella oxytoca* through saturated silica sand. *Ground Water*, 35: 575.
15. Mays, D.C. and Hunt, J.R. (2005) Hydrodynamic aspects of particle clogging in porous media. *Environ. Sci. Technol.*, 39 (2): 577.
16. Deb, A.K. (1969) Theory of sand filtration. *Proc. ASCE, J. Sanitary Eng.*, 95: 399.
17. Hunt, J.R., Hwang, B.C., and McDowell-Boyer, L.M. (1993) Solids accumulation during deep bed filtration. *Environ. Sci. Technol.*, 27: 1099.
18. Ives, K.J. (1961) Filtration using radioactive algae. *Proc. ASCE, J. Sanitary Eng.*, 87: 23.